

## A TUNABLE EIGHT-WAVELENGTH TERAHERTZ MODULATOR BASED ON PHOTONIC CRYSTALS

K. Ji, H. Chen <sup>\*</sup>, W. Zhou, Y. Zhuang, J. Wang

Nanjing University of Posts and Telecommunications,  
Nanjing 210023, China; e-mail: chhm@njupt.edu.cn

*We propose a tunable eight-wavelength terahertz modulator based on a structure of triple triangular lattice photonic crystals by using photonic crystals in the terahertz regime. The triple triangular lattice was formed by nesting circular, square, and triangular dielectric cylinders. Three square point defects were introduced into the perfect photonic crystal to produce eight defect modes. GaAs was used as the point defects to realize tunability. We used a structure with a reflecting barrier to achieve modulation at high transmission rate. The insertion loss and extinction ratio were 0.122 and 38.54 dB, respectively. The modulation rate was 0.788 dB. The performance of the eight-wavelength terahertz modulator showed great potential for use in future terahertz communication systems.*

**Keywords:** terahertz wave, modulator, photonic crystals, eight-wavelength, tunable.

## ПЕРЕСТРАИВАЕМЫЙ ВОСЬМИВОЛНОВЫЙ ТЕРАГЕРЦОВЫЙ МОДУЛЯТОР, ОСНОВАННЫЙ НА ФОТОННЫХ КРИСТАЛЛАХ

K. Ji, H. Chen <sup>\*</sup>, W. Zhou, Y. Zhuang, J. Wang

УДК 548.0

Нанкинский университет сообщений и телекоммуникаций,  
Нанкин 210023, Китай; e-mail: chhm@njupt.edu.cn

(Поступила 2 июня 2016)

*Предложен перестраиваемый восьмиволновый терагерцовый модулятор, основанный на структуре тройных треугольных решеточных фотонных кристаллов, с использованием фотонных кристаллов в терагерцовом режиме. Тройная треугольная решетка сформирована путем размещения круглых, квадратных и треугольных диэлектрических цилиндров. В идеальный фотонный кристалл введены три дефекта с квадратными точками для создания восьми дефектных мод. GaAs использован в качестве источника точечных дефектов для реализации перестраиваемости. Использована структура с отражающим барьером для достижения модуляции при высокой скорости передачи. Коэффициенты вносимых потерь и экстинкции 0.122 и 38.54 дБ. Скорость модуляции 0.788 дБ. Производительность восьмиволнового терагерцового модулятора показала большой потенциал для использования в терагерцовых системах связи.*

**Ключевые слова:** терагерцовая волна, восьмиволновый перестраиваемый модулятор, фотонные кристаллы.

**Introduction.** Recently, demand has increased rapidly for wider bandwidth in short-range wireless communication systems. In such systems, using terahertz (THz) wavelengths is advantageous because they provide broad bandwidth, good directivity, and large information capacity. Therefore, THz communications is a promising direction for short-distance wireless communication systems [1–3]. In THz-wavelength division multiplexing communication systems, a multi-wavelength THz modulator modulates and transmits the THz wave, and this modulator determines the transmission capacity and speed. Research on THz modulators is important both in science and in application [4]. Recently, single-wavelength [5], dual-wavelength [6], and quadruple-wavelength [7] THz modulators based on photonic crystals (PCs) have been proposed.

PCs have the properties of a photonic band gap and photonic localization. PCs, because they are a new type of artificial electromagnetic material, enable the control of THz waves [8, 9]. Here we propose a tunable eight-wavelength THz modulator based on a triple triangular PC, which can modulate eight THz wavelengths. Such a device possesses much greater communication capacity than earlier devices. Simulations show that the present THz modulator has low insertion loss and high extinction ratio.

**Calculation.** Figure 1 shows a PC with a triple triangular lattice. This PC is formed by a triangular array of dielectric cylinders consisting of circular cylinders with radius  $r$ , square cylinders with side length  $w$  and rotation angle  $\theta$ , and triangular cylinders with base length  $w_1$  and height  $g$ . The lattice constant is  $a$ . The dielectric cylinders are made of Si, and the substrate is air. The refractive indices of Si and air are assumed to be 3.418 and 1, respectively.

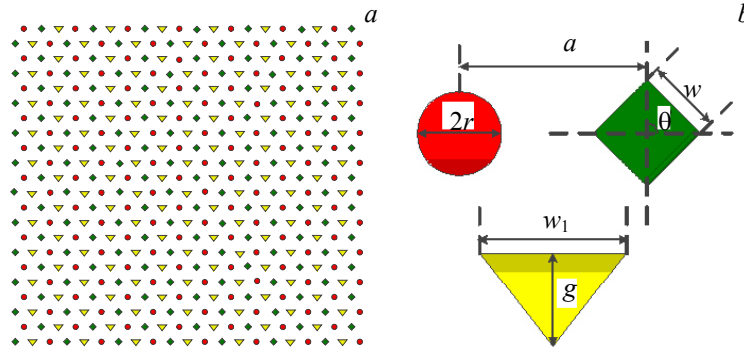


Fig. 1. The structure of triple triangular lattice PC (a) and unit cell of the triple triangular lattice PC (b).

Choosing the appropriate parameters for the triple triangular lattice PC can maximize its photonic band gap. The parameters of the THz modulator are set to  $r = 13.9393 \mu\text{m}$ ,  $w = 25.0909 \mu\text{m}$ ,  $\theta = 45^\circ$ ,  $w_1 = 41.8181 \mu\text{m}$ ,  $g = 30.6666 \mu\text{m}$ , and  $a = 92 \mu\text{m}$ .

Figure 2 shows the band gap of the PC. The normalized frequency of the band gap is 0.326–0.422, and the corresponding frequency is 1.06–1.70 THz. The band gap is larger than those of PCs with simple [5] or compound lattices [7]. As such, by choosing appropriate line defects as waveguides, a larger range of THz wavelengths can propagate through the PC.

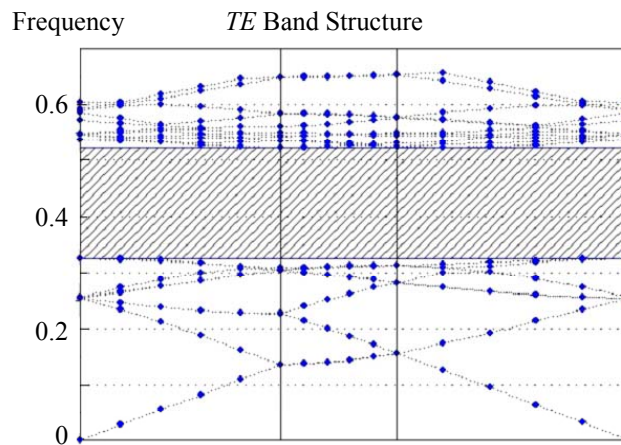


Fig. 2. The band gap of triple triangular PC.

A structure with a reflecting barrier is used to improve the transmission rate of the modulated THz wavelengths. As shown in Fig. 3,  $S_{+i}$  ( $i = 1, 2, 3, 4$ ) is the amplitude of the input wave into the point-defect cavity, and  $S_{-i}$  ( $i = 1, 2, 3, 4$ ) is the amplitude of the output wave.  $r$  and  $r_4$  are attenuation coefficients.

By  $dA/dt = i\omega_0 A - (2\gamma + \gamma_4)A + (2\gamma)^{1/2}(S_{+1} + S_{+2})$ , it can be shown that

$$S_{+1} = [i(\omega - \omega_0)A + (2\gamma + \gamma_4)A](2\gamma)^{1/2} - S_{+2}. \quad (1)$$

Here,  $A$  is the amplitude of the wave in the point-defect cavity, and

$$S_{-4} = (2r_4)^{1/2}A, \quad (2)$$

$$S_{+2} = S_{+3}e^{j\phi} = S_{-2}e^{j2\phi} = (S_{+1} - (2\gamma)^{1/2}A)e^{j2\phi}. \tag{3}$$

$S_{+1}$  can be derived from Eqs. (1)–(3) as

$$S_{+1} = \{[i(\omega - \omega_0)A + (2\gamma + \gamma_4)A]/(2\gamma)^{1/2} + (2\gamma)^{1/2}Ae^{j2\phi}\}/(1 + e^{j2\phi}). \tag{4}$$

The corresponding transmission rate is defined as

$$T = |S_{-4}/S_{+1}|^2 = |(4\gamma\gamma_4)^{1/2}(1 + e^{j2\phi})/[i(\omega + \omega_0)A + (2\gamma + \gamma_4) + 2\gamma e^{j2\phi}]|^2. \tag{5}$$

If  $\omega = \omega_0$ ,  $2\phi = 2m\pi$  ( $\phi = m\pi$ ,  $m = 1, 2, \dots$ ), we obtain that

$$T = 1/[1/2 + (\gamma/\gamma_4 + (1/16)\gamma_4/\gamma)] \leq 1. \tag{6}$$

The transmission rate can be improved by changing the distance between the reflecting barrier and the point-defect cavity.

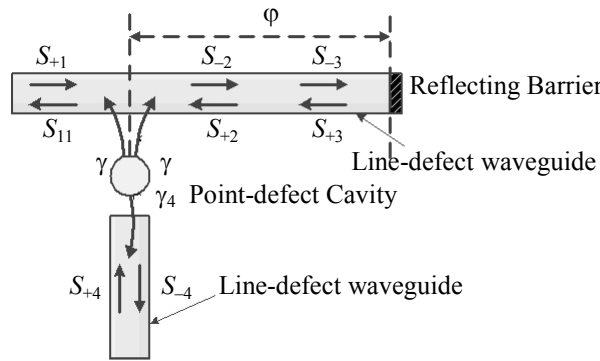


Fig. 3. Structure with a reflecting barrier.

Figure 4 shows the structure of the eight-wavelength THz modulator, showing the three square point defects introduced in the PC as point-defect cavities. Different square point defects produce defect modes with different wavelengths, so we changed the side length and rotation angle of square point defects to produce different defect modes. The number of defect modes produced by square point defects is also related to the side length and rotation angle of the square point defects. The side length of square point defect 1 is 2.712 times that of the square dielectric cylinders, and its rotation angle is 35°. The side length of square point defect 2 is 2.5 times that of the square dielectric cylinders, and its rotation angle is 45°. The side length of square point defect 3 is 2.57 times that of the square dielectric cylinders, and its rotation angle is 40°. The three square point defects produce a better distribution of multiple defect modes, as shown in Fig. 5a. Overall, the transmission rate can be improved by adjusting the locations of the line defect waveguides and the reflecting barrier.

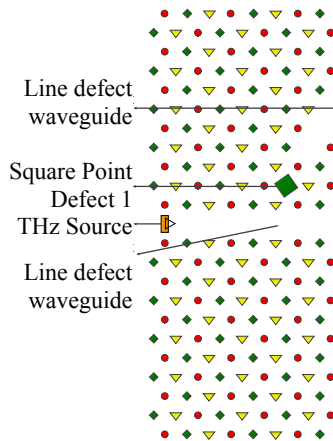


Fig. 4. Structure of the eight-wavelength THz modulator.

The square point defects are gallium arsenide (GaAs) [10, 11], which allows for tunability. The refractive index of GaAs is  $N = n - in'$ , where  $n$  is the real part of  $N$ , and  $n'$  is the imaginary part of  $N$ . If no pump light is applied to GaAs, then  $n$  is 3.55,  $n'$  is 0, and the point defects produce defect modes. Figure 5a shows the simulated results of the transmission spectrum. The blue, green, and red lines correspond to square point defects 1, 2, and 3, respectively. The defect modes have nine wavelengths: 212.9, 218.58, 238.8, 197.71, 205.92, 224.04, 202.82, 210.29, and 229.5  $\mu\text{m}$ , respectively. We selected eight wavelengths with good transmission rates: 218.58, 238.8, 197.71, 205.92, 224.04, 202.82, 210.29, and 229.5  $\mu\text{m}$ . When the wavelength of the incident THz wave is equal to the wavelength of the defect mode, the THz wave can propagate through the modulator, and thus the modulator is in the “on” state.

When 810-nm pump light with an intensity of  $0.4 \mu\text{J}/\text{cm}^2$  is applied to the square point defects, the GaAs is excited and  $n'$  changes to 2.55 [10]. Figure 5b shows the transmission spectrum of the THz modulator. In this case, all the defect modes disappear and thus the THz modulator is in the “off” state.

These results show that the state of the modulator can be controlled by changing the pump light applied to the square point defects.

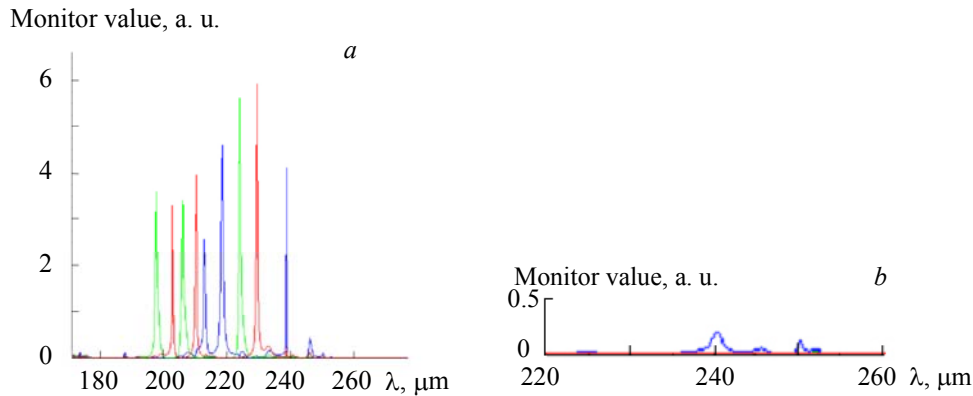


Fig. 5. Transmission spectrum of the THz modulator without (a) and with pump light (b).

**Results and discussion.** The extinction ratio, insertion loss, and modulation rate are important characteristics of modulators. The extinction ratio is defined as

$$\eta = 10\log(I_{\max}/I_{\min}), \quad (7)$$

where  $I_{\max}$  and  $I_{\min}$  are the maximum and minimum intensities of the transmitted THz wave after modulation, respectively, and  $\eta$  is the extinction ratio of the modulator.

The insertion loss is defined as

$$\gamma = 10\log(I_{\text{in}}/I_{\max}), \quad (8)$$

where  $I_{\text{in}}$  is the intensity of the THz wave without modulation, and  $\gamma$  is the insertion loss of the modulator.

The modulation rate is defined as

$$\nu = 1/T, \quad (9)$$

$$T = T_1 + T_2, \quad (10)$$

where  $\nu$  is the modulation rate of the modulator,  $T_1$  is the response time of the change in  $n'$  ( $T_1$  is about 100 ps [11]),  $T_2$  is the stability time of the modulator, and  $T$  is the sum of  $T_1$  and  $T_2$ .

Figure 6 shows the case where the THz source inputs eight THz waves whose wavelengths are consistent with the defect modes, revealing the time-domain steady-state responses of the “on” and “off” states. Figures 6a,c,e show time-domain steady-state responses of the “on” state detected by the first, second, and third detectors, respectively. Figures 6b,d,f show the time-domain steady-state responses of the “off” state detected by the first, second, and third detectors, respectively.

Here,  $I_{\max}$  is the sum of the values of Fig. 6a,c,e, and  $I_{\min}$  is the sum of the values of Fig. 6b,d,f. From Fig. 7 we obtain that  $I_{\max}$  and  $I_{\min}$  are 7.7788 and  $1.08746 \times 10^{-3}$ , respectively;  $T_2$  is  $1.1687 \times 10^{-9}$  s, and  $I_{\text{in}}$  is 8. From Eqs. (7), (8), and (10) the extinction ratio is calculated as 38.54 dB, the insertion loss as 0.122 dB, and the modulation rate as 0.788 GHz. The insertion loss is lower, and the extinction ratio 56 is higher compared with earlier results.

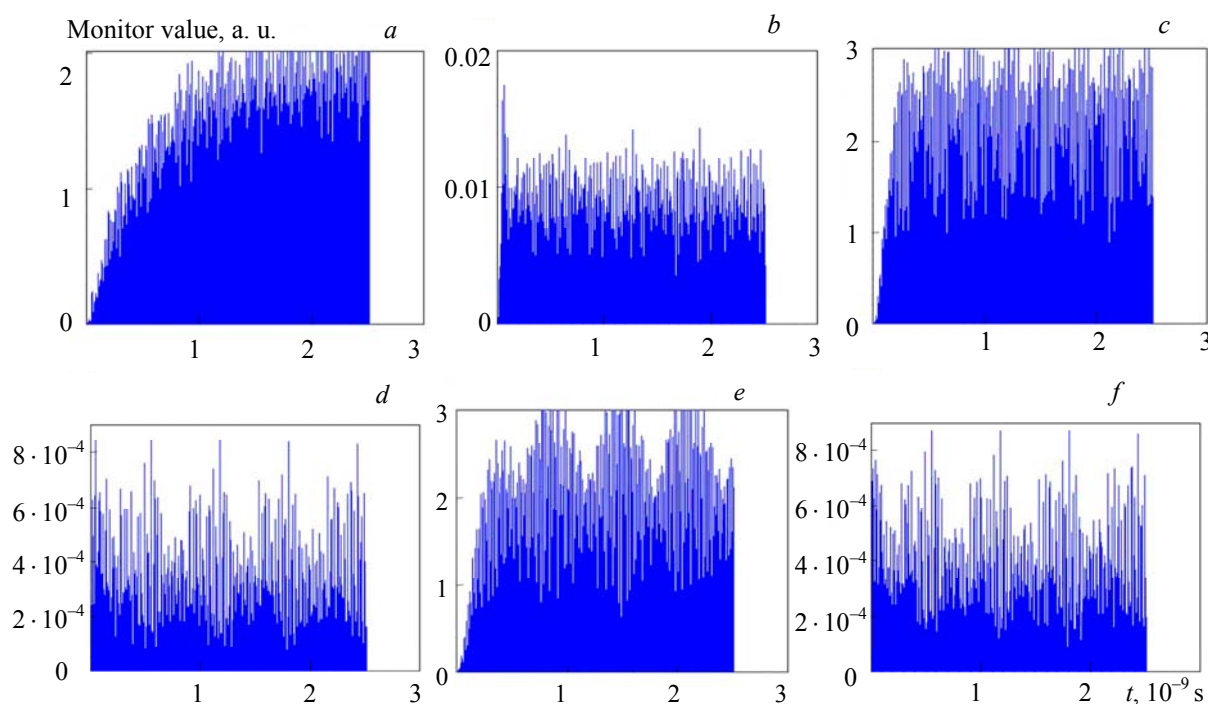


Fig. 6. Time-domain steady-state responses of “on” state detected by (a) detector 1, (c) detector 2, and (e) detector 3; Time-domain steady-state responses of “off” state detected by (b) detector 1, (d) detector 2, and (f) detector 3.

Figure 8 illustrates the steady-state THz field intensity distribution of the THz modulator, showing that the eight THz waves can be modulated effectively when they are inputted simultaneously.

**Conclusion.** We designed a tunable eight-wavelength THz modulator, and simulated results showed that its performance was excellent. Its dielectric cylinders were made of Si. Because Si technology is the most advanced semiconductor technology, this modulator can be produced easily and inexpensively. This THz modulator can modulate eight THz wavelengths, which greatly expands its communication capacity. This device shows great potential for future use in multi-wavelength, high-capacity THz communication systems.

**Acknowledgment.** This work was supported by the National Nature Science Foundation of China (Project No. 61077084, 61571237) and the Colleges and Universities in Jiangsu Province plans for graduate research and innovation (No. KYLX15\_0835).

## REFERENCES

1. H. Chon, B. A. Ozan, A. F. Ian, *IEEE T. Wirel. Commun.*, **14**, 2402–2412 (2015).
2. J. S. Li, *Opt. Laser Technol.*, **56**, 263–268 (2014).
3. T. Chen, P. Liu, J. Liu, Z. Hong, *Appl. Phys. B*, **115**, 105–109 (2014).
4. L. J. Zhou, W. T. Jiang, *Commun. Tech.*, **47**, 348–353 (2014).
5. H. M. Chen, J. Su, J. L. Wang, X. Y. Zhao, *Opt. Express*, **19**, 3599–3603 (2014).
6. L. J. Song, H. M. Chen, X. Y. Zhao, J. L. Wang, *Stud. Opt. Commun.*, **38**, 42–44 (2012).
7. W. Zhou, H. M. Chen, J. L. Wang, *J. Appl. Spectrosc.*, **82**, 788–793 (2015).
8. S. John, *Phys. Rev. Lett.*, **58**, 2486 (1987).
9. E. Yablonovitch, *Phys. Rev. Lett.*, **58**, 2059 (1987).
10. H. F. Tiedje, H. K. Haugen, J. S. Preston, *P. Soc. Photo-Opt. Ins.*, **274**, 187–197 (2007).
11. P. Kuzel, F. Kadlec, H. Nemeč, *J. Chem. Phys.*, **127**, 1–11 (2007).